Original Paper (Invited)

Study of Stay Vanes Vortex-Induced Vibrations with different Trailing-Edge Profiles Using CFD

Alexandre D'Agostini Neto[1], Fábio Saltara[2]

[1]VOITH Hydro
Rua Friedrich von Voith, 825, São Paulo, 02995-000, Brazil,
alexandre.neto@voith.com
[2]Department of Mechanical Engineering, University of São Paulo
Av. Prof. Mello Moraes,2231, São Paulo, 05508-970, Brazil, fsaltara@usp.br

Abstract

The 2D flow around 13 similar stay-vane profiles with different trailing edge geometries is investigated to determinate the main characteristics of the excitation forces for each one of them and their respective dynamic behaviors when modeled as a free-oscillating system. The main goal is avoid problems with cracks of hydraulic turbines components. A stay vane profile with a history of cracks was selected as the basis for this work. The commercial finite-volume code FLUENT® was employed in the simulations of the stationary profiles and, then, modified to take into account the transversal motion of elastically mounted profiles with equivalent structural stiffness and damping. The k-ω SST turbulence model is employed in all simulations and a deforming mesh technique used for models with profile motion.

The static-model simulations were carried out for each one of the 13 geometries using a constant far field flow velocity value in order to determine the lift force oscillating frequency and amplitude as a function of the geometry. The free-oscillating stay-vane simulations were run with a low mass-damping parameter (m*ζ=0.0072) and a single mean flow velocity value (5m/s). The structural bending stiffness of the stay-vane is defined by the Reduced Velocity parameter (Vr).

The dynamic analyses were divided into two sets. The first set of simulations was carried out only for one profile with 2≤Vr≤12. The second set of simulations focused on determining the behavior of each one of the 13 profiles in resonance.

Keywords: Vortex-Induced Vibrations, Stay Vanes, Trailing-Edge Profile

1. Introduction

The problem of Vortex-Induced Vibrations (VIV) in stay vanes is being discussed in literature for more than 40 years, with the first work publication in July of 1965 (Goldwag *et al. Apud* Gummer (1992) [3]). Although this phenomenon is already well known, we cannot say that the VIV are a so uncommon problem, and the verification of the susceptibility of its occurrence on stay-vanes, guide-vanes and turbine runner blades of a new project or of a modernization is mandatory for a reliable design.

The typical scenario of vortex-induced vibration in stay-vanes of hydraulic turbines was described by Gummer *et al* (1992) [3] as some abnormal noise or vibration in the station with the turbine running at loads above approximately 70 per cent guide vane opening in the first hours of a unit operation. In some most critical cases, the turbine operation became restricted before full commercial operation of the unit. In the most part of cases, however, only after a short operating period the inspections revealed cracks in the welds between the vanes and the stayring. The size of the cracks changed with the intensity of the phenomenon,

and their cause is usually attributed to fatigue.

This work aims to show through CFD simulations of both static and a freely oscillating 2-D stay vane profile how the main physical variables (like trailing edge thickness, mass-damping parameter and reduced velocity) can interfere on the main outputs of this problem (exciting force frequency and amplitude, oscillation amplitude and energy transferred from the flow to the structure).

2. Vortices and Flow-Induced Vibrations

In the case of stay-vanes, the trailing-edge profile modification is the most employed solution for eliminating the VIV occurrence. This procedure is adopted due to the fact that the Strouhal number, given by equation (1), remains approximately constant and near some experimentally verified values for a stay-vane in a fixed Reynolds number flow after the modification. Liess (1987) [7] shows some reference Strouhal Numbers for some typical profiles. As a consequence of that, a reduction on the trailing edge thickness would increase the vortex-shedding frequency, which must not be coincident with a flexional or torsional mode.

$$St = \frac{fd_{ref}}{U} \tag{1}$$

Where f = Vortex-Shedding frequency
   d_{ref} = Transversal dimension where the flow separates from the body
   U = free-stream velocity

The general behavior of the von Karman vortex street shed from plates and bodies with sharp trailing edge depends strongly on the main geometry characteristics of their trailing edges (specially on the thickness) and on the flow Reynolds Number. If the body has a blunt trailing edge, the wake will have the same behavior observed in bluff bodies. A good reference for a vortex-shedding model is the one proposed by Gerrard (1966).

Regarding the dynamic model of the vane profiles, a mass-spring-damper system was employed to simulate its transversal displacements (1st vibration mode – bending). For all simulations, the fraction of the critical damping employed was 1% according to the commonly calculated values shown by Gissoni (2005) [9] and the flexional stiffness calculated from the non-dimensional parameter called Reduced Velocity ($V_r=U/(f_n d_{ref})$, being f_n the natural frequency of the body). The model can be described by the one dimensional linear mechanical system equation (2).

$$m\,\ddot{y} + c\,\dot{y} + k\,y = F_y \tag{2}$$

With the addition of the Lift Coefficient (Cl), the additional fluid-displaced mass (m_d), the mass parameter ($m^*=m/md$), the reduced velocity parameter (Vr), the structural damping (ζ), the dimensionless displacement ($Y=y/d_{ref}$) and the dimensionless time ($\tau=t/T_n$, where T_n is the structure natural period of oscillation, Tn=1/f_n) we have finally the equation (3), where the lift coefficient is obtained from the integration of the projected pressure field on the y direction (transversal to the flow) over the profile surfaces.

$$\ddot{Y} + 4\pi\zeta\sqrt{1+\frac{1}{m^*}}\dot{Y} + 4\pi^2\left(1+\frac{1}{m^*}\right)Y = C_l\,\frac{2V_r^2}{m^*\pi} \tag{3}$$

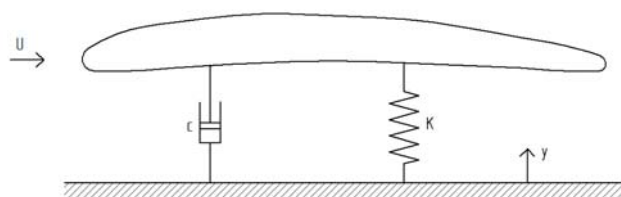Fig. 1 shows an illustration of the considered model.

Fig. 1 Model used for the simulations of the displacement on the transversal direction of the flow

The energy transferred from the flow to the structure is calculated according to the procedure described by Meneghini (2002) [10]. Considering an excitation force F_l (t) for unitary length of the foil, by definition, the energy transferred per cycle to the oscillating body will be given by:

$$\overline{E} = \int_0^T F_l(t)dy \tag{4}$$

Being the exciting force and the displacement modeled by:

$$F_l = \frac{1}{2}\rho U^2 b \overline{C_l}\sin(2\pi f t + \varphi) \tag{5}$$

$$y = A\sin(2\pi f t) \tag{6}$$

where b is the stay vane length, t is the current time and φ the phase angle between the body displacement and lifting force. The energy transferred from the flow to the system in each period step T of oscillation is given by:

$$\overline{E} = \int_0^A F_l dy = \int_0^T F_l \frac{dy}{dt}dt \tag{7}$$

Which in a non-dimensional form will be:

$$E = \frac{\overline{E}}{\frac{1}{2}\rho U^2 b^2} = -\pi \overline{C_l}\left(\frac{A}{b}\right)\sin\varphi \tag{8}$$

Thus, the energy transferred from the flow to the structure is proportional to the sine function of the phase angle between the displacement and the force acting on the body.

Regarding the oscillation amplitude and the *lock-in*, according to Blevins (1990) [13], when there is a free-oscillating body immersed in a flow and increasing its reduced velocity (V_r), it can be observed that the vortex-shedding frequency will increase linearly with this parameter until it reaches the natural frequency of the body (or a value near to that frequency). The *lock-in* phenomena means that, for certain conditions of the $m*$ parameter, as the V_r is increased, the vortex-shedding frequency (f) becomes close to the natural frequency of the structure (f_n) and the two frequencies synchronize for a large range of V_r. The vibration amplitude usually resulting from this phenomenon is relatively high. Continuing raising the V_r parameter makes the shedding frequency increase again with the same linear tendency line that it was rising before, remaining progressively with the characteristics of a non-oscillatory regime. Fig. 2 shows the *lock-in* phenomenon for freely oscillating cylinders with different mass parameter $m*$. It is important to see that the tendency of $f*$ (vortex-shedding frequency/natural frequency) remaining close to 1.0 (*lock-in*) changes with $m*$.
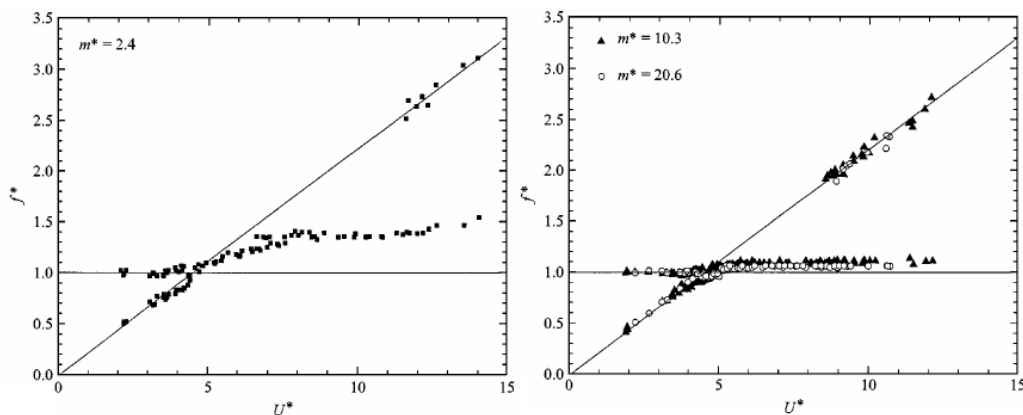

Fig. 2 $f*$ parameter response to V_r ($U*$ for this author$)$ variation for freely oscillating circular cylinders with different mass-parameter $m*$ values (Khalak, 1999 [6])

3. Numerical Method and Methodology

As it was already mentioned, a 2-d profile of a stay-vane with a history of cracks was adopted in this work. Miyagawa *et al* (2004) [8] made a comparison of simulating this phenomena with 2-d or 3-d models (with RANS turbulence modeling and LES), and the final conclusion was that both 2-d and 3-d simulations had good agreement with experimental results. The original profile is shown in Fig. 3, and has a total 32mm thickness on the trailing edge. This profile will be in this paper identified as Profile 1.
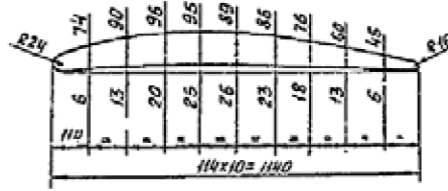
Fig. 3 Stay-Vane Profile used as basis for this work

The simulations can be divided mainly in three groups - one for stationary profile with different geometries and other two for dynamic profiles in different conditions, as follows:

- Stationary base profile with 13 different trailing edge geometries simulations with same boundary conditions;
- Freely oscillating original profile simulated for $2 \leq V_r \leq 12$, but, in this case, with only one trailing-edge geometry. For this V_r range, the resonance or the *lock-in* (if it occurs) can be observed;
- Simulations of the vortex-emitting profiles in resonance with the vortex-shedding exciting force. In other words, the structural stiffness was set to a value that made the natural frequency of the system equal to the vortex-shedding frequency.

For the simulations of the freely oscillating profile, a deforming mesh technique was employed. In deformable meshes, the edges (faces, in 2D cases) are idealized as interconnected springs. The original configuration of the mesh is idealized as the equilibrium state of it. For ensuring the mesh quality, when displacements are large when compared to original cell sizes, new elements are created (remeshing). The integral form of the conservation equation for a general scalar ϕ used by the simulation program is corrected with the grid velocity of the moving mesh (u_g).

$$\frac{d}{dt}\int_V \rho\phi dV + \int_{\partial V} \rho\phi\left(\vec{u} - \vec{u}_g\right) \cdot d\vec{A} = \int_{\partial V} \Gamma\nabla\phi \cdot d\vec{A} + \int_V S_\phi dV \tag{9}$$

In order to keep the boundary layer volumes quality and geometry, a rigid-body zone was created enclosing the profile, which means that the stay-vane plus a region near the boundary layer have a rigid body motion without any kind of distortion. In the exterior region, the elastic model described previously was employed with remeshing.

Simulations without any kind of dynamic meshes were held with a second-order scheme for time discretization. Simulations with dynamic meshes were performed with a first-order time scheme and a smaller time-step. The cell fluxes were calculated through the second order UPWIND method for all the cases.

The dynamic model was implemented on the profile through a code that solves the system described by the equation 3 and gives as output the profile position after each time step. The pressures integrated over the body surfaces are used as the force input to solve the body displacement equations.

4. Results

- First Simulations Set

Initially, in order to determinate the best model for simulating the problem some simulations were carried out with different parameters, such as the main domain geometry, the time-step, the elements geometry and the turbulence model for the original profile in order to validate the results with the reference. As a result of this whole set of simulations, the final mesh (Fig. 4 for profile 1) and other simulation parameters were set and remained constant for all the other cases. The detailed results comparing all parameters are not going to be shown in this paper, but the final mesh had approximately 50000 volumes for all cases, the k-ω SST turbulence model was adopted and a time-step of 1×10^{-4}s has been set. Also the k-ε and the *standard k-ω* models were evaluated. Several references shows that the k-ε model fails to predict the near-wall flow with adverse pressure gradient, which characterizes flows with a separation region. One of them is Bradshaw (*apud Wilcox(1993)* [14]). It is shown that for a flat plane with adverse pressure gradient, the predicted skin friction with *standard k-ω* exceeds only 5% the experimentally measured value, and the one with the k-ε model exceeds by as much as 20%. As a main consequence, the vortex-shedding frequency calculated with the k-ε model was lower when compared to the final model. Also the standard k-ω model is problematic in the treatment of the non-turbulent free-stream boundaries due to the fact that it requires non-physical boundary conditions on ω and the flow becomes very sensitive to this value. The k-ω SST model was finally selected due to the fact that it combines the good near-wall treatment of the standard k-ω model and the good behavior of the k-ε model away from walls using a blending function.
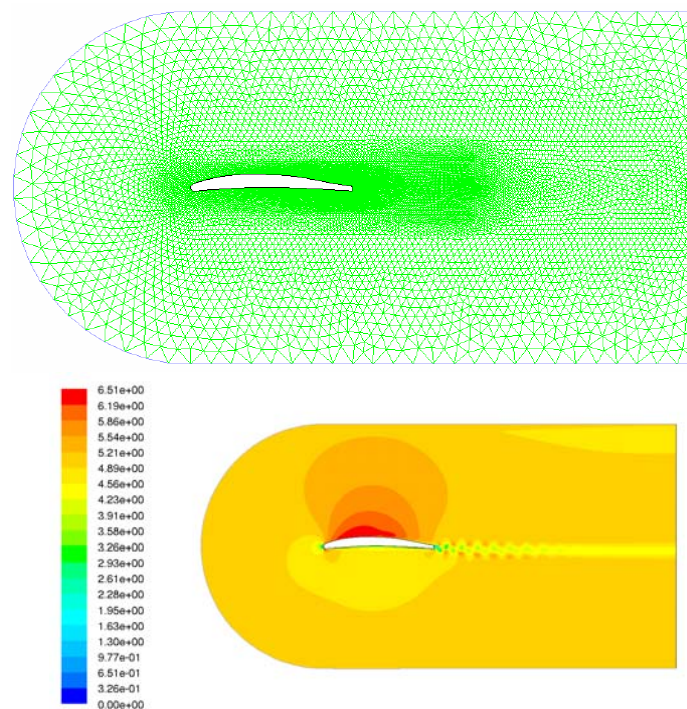

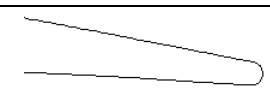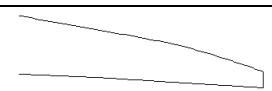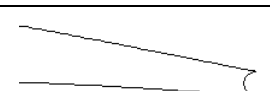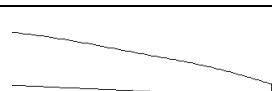**Fig. 4** Mesh adopted for simulations and velocity contours for Profile 1
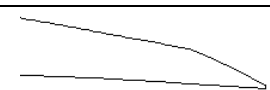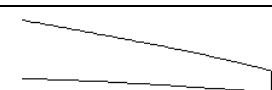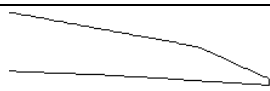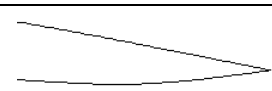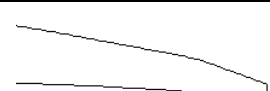
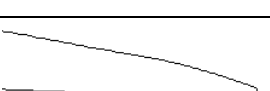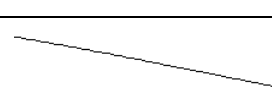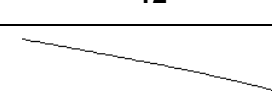Being determined the computational model for solving the problem, the influence of the trailing edge profile was evaluated through 13 different geometries adopted for the same vane. The PRESSURE OUTLET boundary condition was used downstream in the flow and the VELOCITY INLET in the entrance region. The temporal series of the lift coefficient (C_l) was obtained as main output.

As it was mentioned before, the profile shown in Fig. 3 was adopted as the main reference for this work (#1). Profile 2 came from a variation that was executed by the original manufacturer of the turbine in site for this same profile in order to try to solve the cracks problem. It has the same thickness of the first one, but with different geometry. For profiles 3 to 9 the trailing edge thickness was reduced with the execution of a chamfer starting over the same point (corresponding to 90% of the chord line length) on the suction side of

the profile for all cases and ending in variable trailing edge thicknesses. With this procedure, changes with different "abruptness" were obtained. The same criterion was adopted for determining the geometry of profiles 10 to 12, but, in those cases, the geometrical changes are made on the profile pressure side. Finally, profile 13 is similar to profile 1 just making a cut-out on the rounding and making the back face planar.

The main results for all simulations of this first step are shown in Table 1. On this table are presented the general form of the profiles, their respective thicknesses of the trailing edge, the Lift Coefficient amplitude and the vortex-shedding frequency. A typical temporal signal for the lift coefficient is shown in Fig. 5.

Table 1 – Resume of the main data of the 1st phase simulations

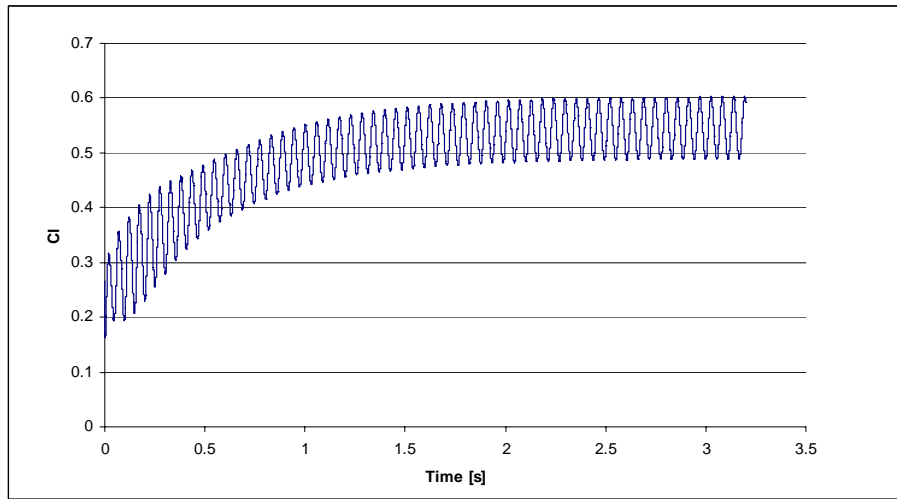| Profile	Thck (mm)	Cl Amp	Freq (Hz)	Profile	Thck (mm)	Cl Amp	Freq (Hz)
1	32	0.013	34.96	7	20	0.019	40.32
2	32	0.031	29.41	8	24	0.036	34.60
3	4	0.000	0.00	9	28	0.057	31.44
4	8	0.000	0.00	10	0	0.000	0.00
5	12	0.000	0.00	11	16	0.026	43.47
6	16	0.000	0.00	12	24	0.049	34.97
				13	32	0.072	30.12

Fig. 5- Typical Cl variation with the time

Comparing cases 1 and 2, it can be seen that the modification in the geometry caused only a little variation of the shedding frequency and huge increase on the *Cl* amplitude. This can be explained by the increase of the vortices intensity with the geometrical change that induces a "stronger" variation in the pressure field near the profile surfaces. Fig. 6 shows the vorticity field for each profile where the differences can be clearly seen. For cases 3, 4, 5, 6, 7, 8 and 9 two main effects can be observed. One of them is just the expected increase of the vortex-shedding frequency with the reduction of the trailing edge thickness (7, 8 and 9) and the corresponding decrease of the lift-coefficient amplitude. The other one is that for some cases an alternating vortex street has not been formed due to the chamfer geometry, according to Fig. 7. In the model proposed by Gerrard for vortex shedding, for the formation of a vortex street it is necessary that the opposites shear layers (with opposites vorticity signals) interacts between each order to form the vortices that will be advected downstream in the flow. In the cases 3, 4, 5 and 6, it is possible to see that the separation in the suction side just occurred in the point where the chamfer started due to the sudden geometry change. In those cases, the transversal distance between the separation points and, therefore, between the both shear layers acts like a barrier for the formation of a vortex street. Fisher *et al* (1994) [2] shows through experimental results that the vortex-shedding frequency after executing a trailing edge thickness reduction became lower than the value measured of it for the blunt trailing edge due to the same phenomena retracted here. Taking in account the Strouhal number, it is possible to predict that the frequency will be smaller by using the correct separation points distance as reference dimension (d_{ref}), and not the trailing edge thickness itself. For the cases 10, 11, 12 and 13 it is important to note that the expected behavior of the vortex-shedding frequency was obtained as results due to the fact that the separation point was really the trailing-edge, and not the chamfer execution point itself.

It is also interesting to observe that the cases 6 and 11, 8 and 12 (with the same trailing-edge thicknesses) presented different results due to the chamfer characteristics (Fig. 8).

The difference between profiles 1 and 13 is that the separation point is a little downstream at the rounding, and not in the region of the trailing-edge where the dimension is effectively 32mm (which occurs on case 13), as it can be seen in Fig. 9.
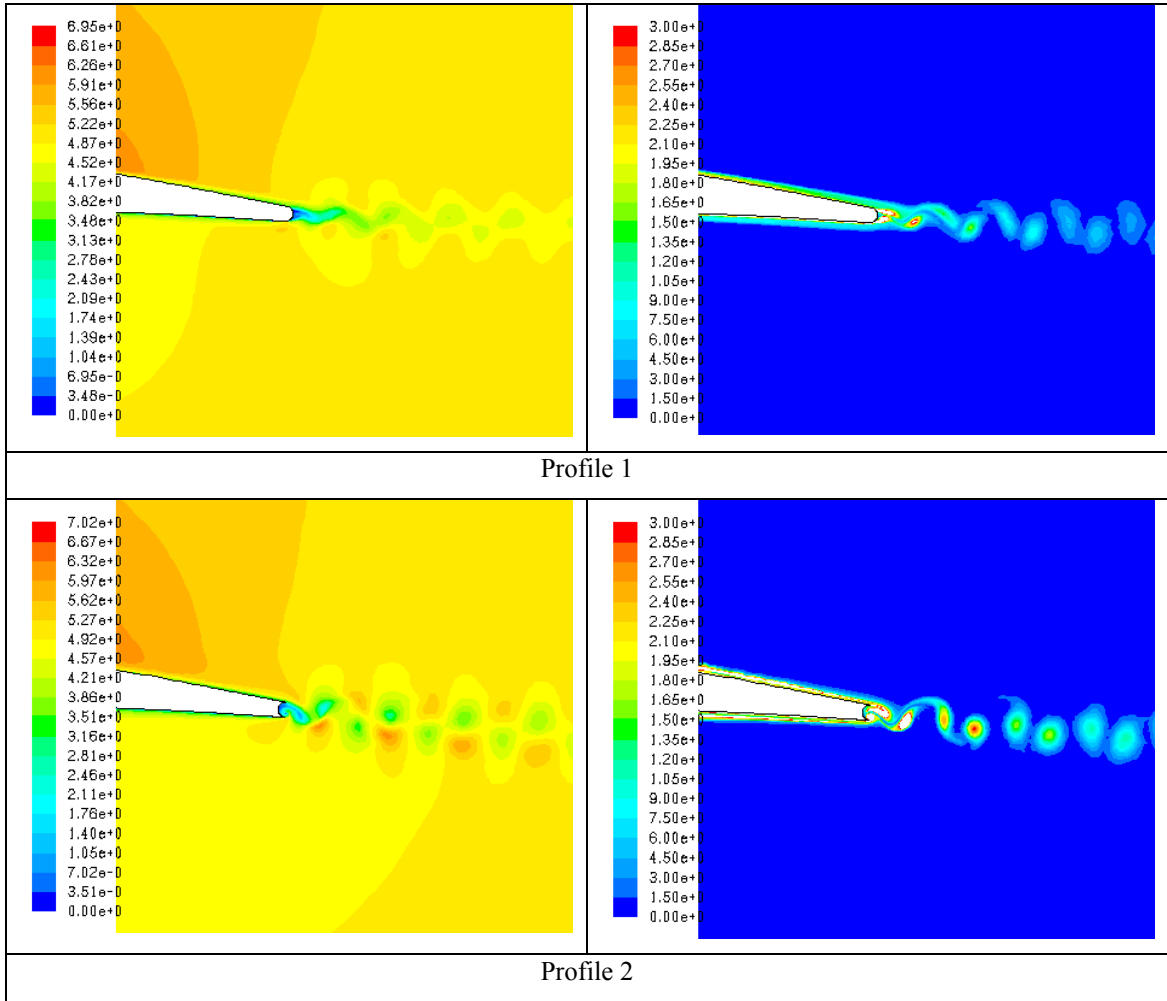
Profile 1

Profile 2

Fig. 6 – Velocity [m/s] and vorticity [1/s] fields for profiles 1 and 2
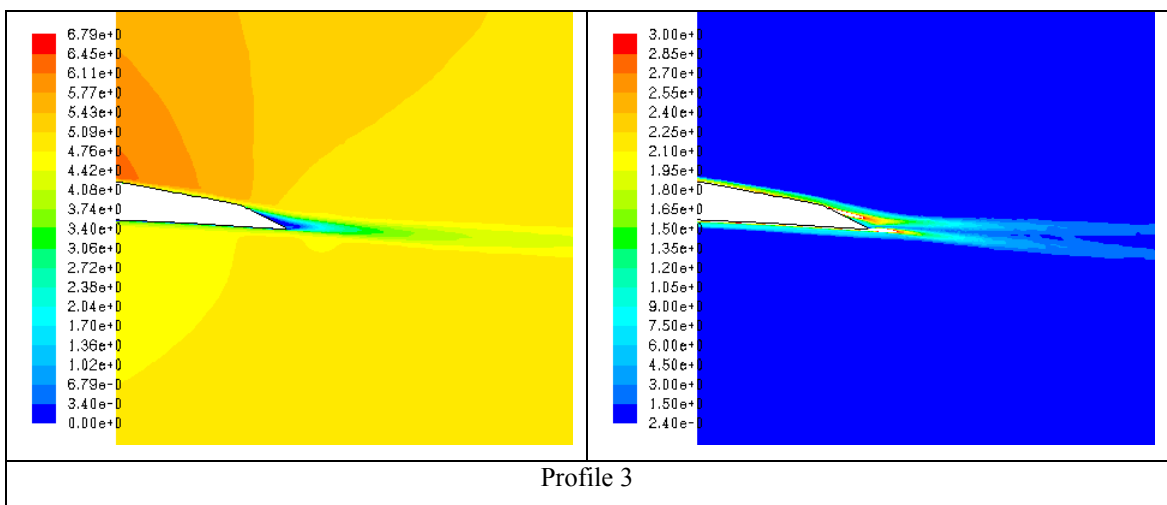

Profile 3

Fig. 7 - Velocity [m/s] and vorticity [1/s] fields for profile 3 – Flow Separation in the chamfer region
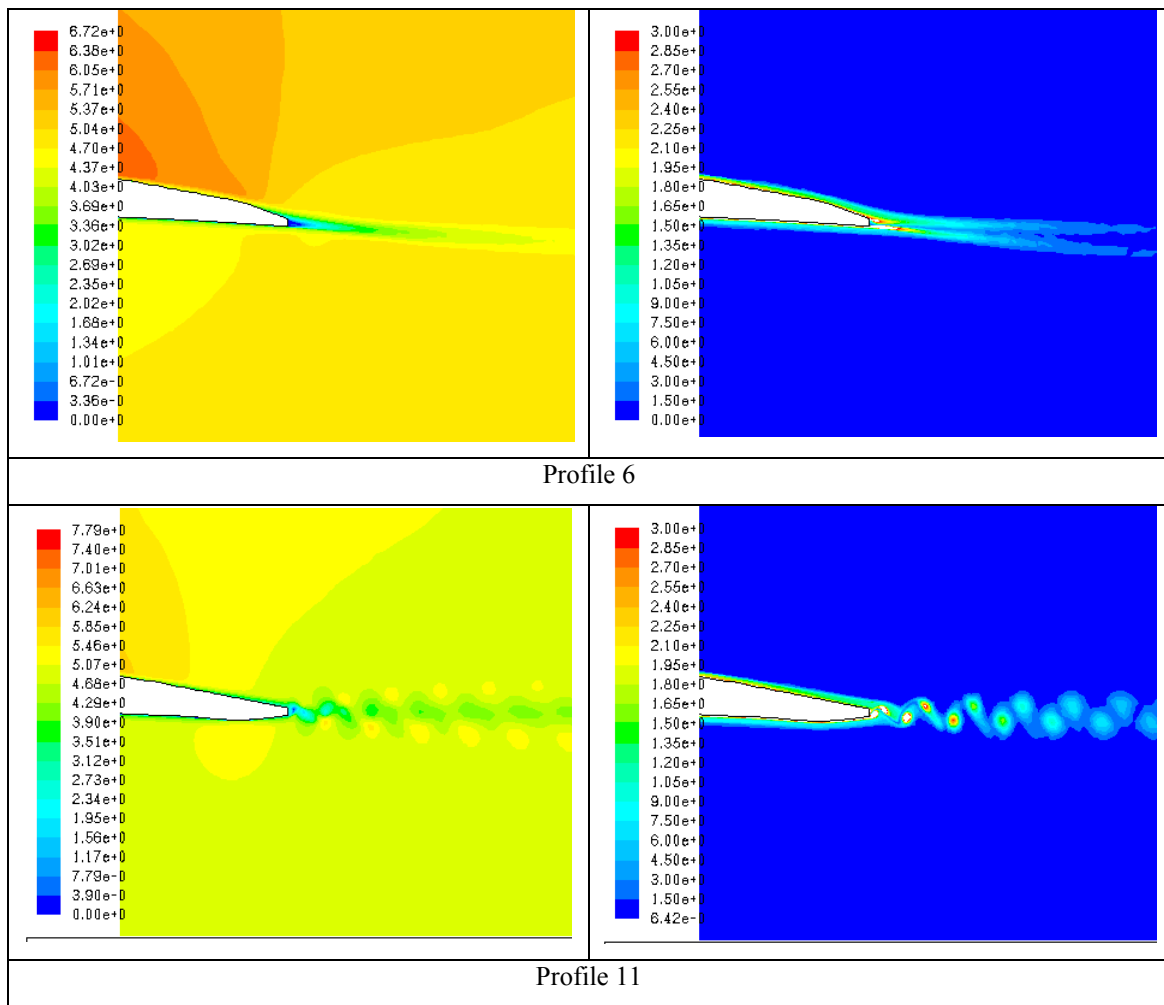
Fig. 8 – Profile 6 X Profile 11 – The same trailing edge thicknesses with chamfers from the suction and pressure sides respectively

Fig. 9 – Details of the separation region for profiles 1(velocity vectors [m/s]) and 13 (vorticity contours [1/s]). Note the same geometrical thickness, but different dimension for the effective separation point (profile 13 "thicker" than profile 1 for the separation point, that explains the higher shedding frequency of profile 1).

371

- Second Simulations Set

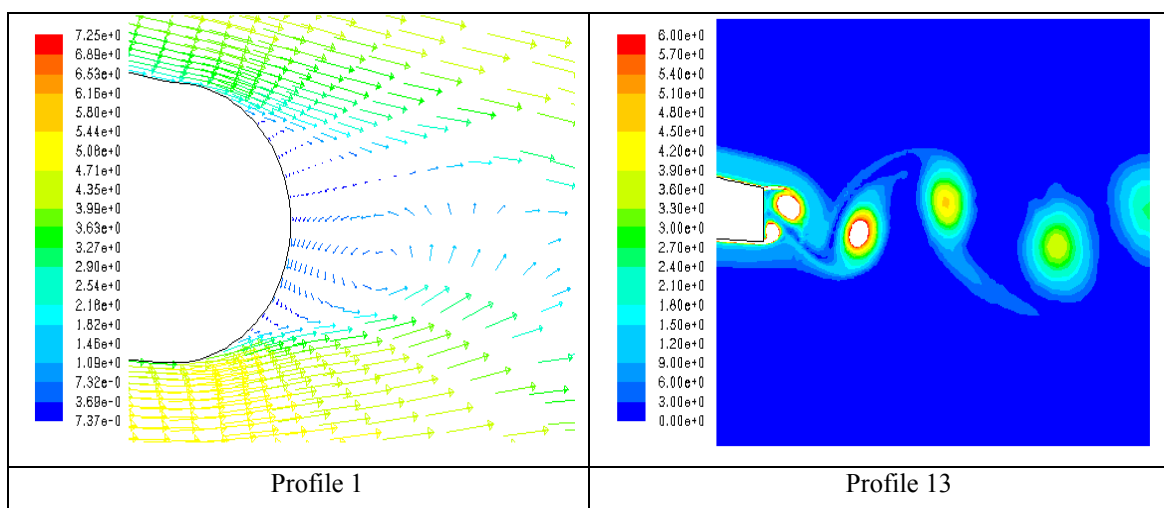As it was already mentioned, an additional code coupled with the main finite-volume solver was employed to calculate the profile displacements in the time (UDF – User-Defined Function). For all the dynamic simulations from now, the mass parameter (m^*) adopted will be 0.72.

This simulation phase consists in evaluating the vibration amplitude for the profile 1 in the range of reduced velocities where the *lock-in* phenomenon can occur ($2 \leq V_r \leq 12$). The main boundary conditions remained constant, and the variation of the V_r parameter was given by changes in the structural stiffness. In other words, from the definition of the V_r parameter, a structure with a lower reduced velocity value would be less stiff then one with a higher value. Fig. 10 shows the amplitude [m] and the f^* (relationship between vortex shedding frequency and natural frequency of the body) parameter as a function of V_r.
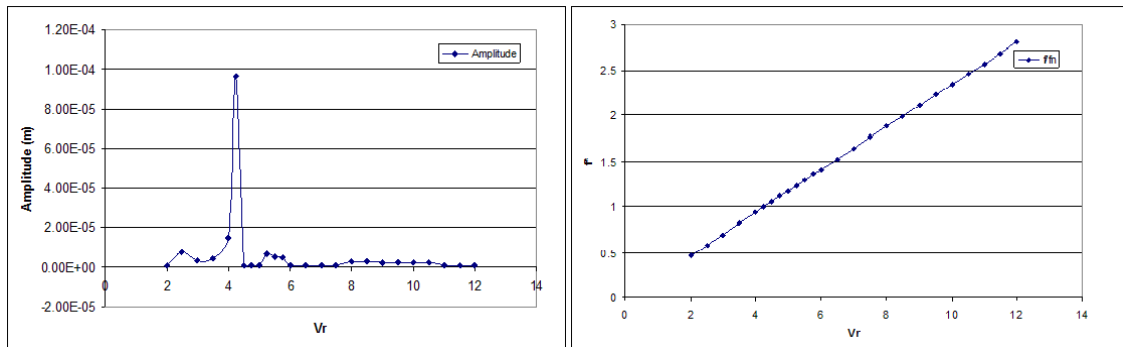

Fig. 10 – Oscillation Amplitude and f^* parameter for profile 1 as functions of V_r

As it can be observed, the corresponding reduced velocity values for the peak amplitude and for $f^*=1$ is the same, which was already expected. It wasn't observed a *lock-in* in this range of reduced velocities for this vibration mode, but, as it could be seen in Fig. 2 it can be explained by the very-low mass parameter m^* of the stay vane associated to it. Mainly, the characteristics of a resonant body were only observed. Hesketad *et al* found as experimental results the same amplitude and f^* behaviors for models with different trailing edges profiles and also Miyagawa *et al* (2004) [8] found the same behavior for the Amplitude x V_r curve of a profile, but with the peak amplitude for $Vr=6$. Also in additional works for flat planes (Chen [12]), it has already been demonstrated that the geometry is hugely responsible for this phenomena characterization.

Finally for this simulation phase, the energy transferred from the flow to the structure per cycle is shown in Fig. 11
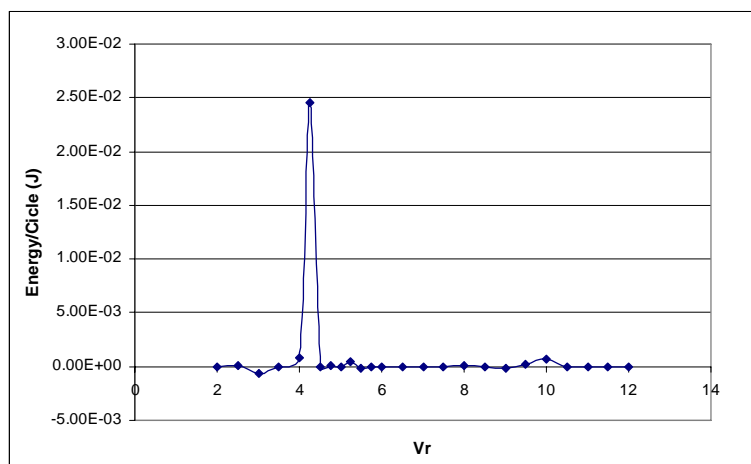

Fig. 11 – Energy transferred from the flow to the structure in a cycle

- Third Simulations Set

Finally, for this last set of simulations, in order to compare the behavior of the vortex-emitting profiles in resonance, several cases were simulated considering that, for each profile, the reduced velocity variation range was +/- 1 with the mean value being the one which takes the stay-vanes into resonance. This mean value can be determined through the Strouhal number (in this case, considered 0.22 for all profiles to keep a same expected mean V_r value as the basis) and d_{ref}. So, in this way, it was possible to obtain some curves that shows the variation of the dynamic behavior of the stay vanes in an imposed resonance condition. Fig. 12 shows the oscillation amplitude near the resonance for the vortex-emitting profiles of this work.
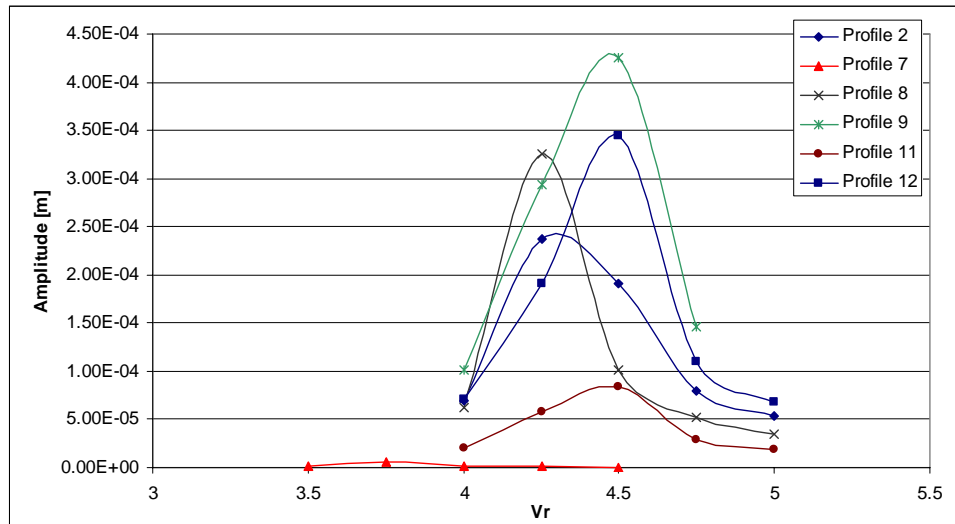

Fig. 12 – Main vortex-emitting profiles in resonance

As it can be observed from Fig. 12, the behavior of each curve changes with the profile geometry. By increasing the trailing-edge thickness (chamfer executed in the suction or in the pressure sides) there is a corresponding increase in the oscillation amplitude. Taking in account the dimensionless parameters used for describing the VIV and the structure, a profile with a thicker trailing-edge (with a lower vortex-shedding frequency) would need to be also more flexible that one with a sharper trailing-edge for being in resonance maintaining fixed the far flow speed. Therefore, an increase of the oscillation amplitude can be explained both by a combination of the increase intensity of the vortex-street (shown in the first set simulations by the lift-coefficient amplitude) and a reduction of the structural stiffness with the increase of the trailing-edge thickness. In other words, considering two stay-vanes with the same profiles, but a longer one with a thicker trailing edge and a shorter one with a sharper trailing edge, and being both of them in resonance with the vortex-shedding, the longer one would oscillate with a higher amplitude than the shorter one.

Regarding the energy transferred from the flow to the structure per cycle, also the thicker profiles presented a higher value.

5. Final Considerations

Taking in account the results obtained in this work, some considerations should be made:

- For the static cases, not only the trailing-edge thickness itself determinates the exciting frequency of stay-vanes, but also the way that the geometry changes is relevant due to changes in the separation region;
- About the *lock-in* phenomenon, it was observed that for this model it does not occur even for a wide range of V_r parameter studied here due to the fact that a low m^* was also adopted, that means, a simple resonant condition was identified. For torsional condition the result can change due to the fact that the m^* parameter increases;
- For all the vortex-emitting profiles in resonance, it was observed that the increasing of amplitude with the trailing-edge thickness is caused by the combination of the reduction of the structural stiffness with the increase of the vortex street intensity for the fixed far-flow speed due to the way that the structural properties of the stay-vane are obtained. But also it was verified that for the thicker profiles the energy transferred from the flow to the structure was bigger;

- For the last set of simulations, it can be seen that, for the flexional mode of the stay vanes, the high oscillation amplitude range of the V_r parameter stays within approximately +/-1 of its predicted mean value through the Strouhal number (well defined resonance, without *lock-in* for the flexional mode). In this case, using an imposed Strouhal number of approximately 0.22 (through the d_{ref} variable), the predicted mean V_r value is approximately 4.5.

Nomenclature

b	Stay Vane length	m^*	Mass Parameter [$=m/m_d$]
c	Damping	St	Strouhal Number [$=f^*d_{ref}/U$]
C_l	Lift Coefficient	t	Time
d_{ref}	Transversal reference dimension of separation point	T_n	Structure Natural Period
$\bar{E}$	Energy transferred to oscillating body per cycle	U	Far field velocity
E	Dimensionless $\bar{E}$	U^*	Another Reference for Reduced Velocity (in figure 02)
F_y	Force in transverse direction	V_r	Reduced velocity parameter [$=U/f_n{*}d_{ref}$]
F_l	Modeled exciting force	Y	Dimensionless displacement [$=y/d_{ref}$]
f	Vortex Shedding Frequency	ϕ	General Scalar Quantity
f_n	Body Natural Frequency	φ	Phase angle between displacement and force
k	Structural Stiffness	ρ	Fluid Specific Mass
m	Mass	τ	Dimensionless time[$=t/T_n$]
m_d	Additional fluid displaced mass	ζ	Structural damping

References

[1]D`Agostini N., A., Saltara, F., 2007, "Simulation of vortex induced vibration of pairs of cylinders in tandem arrangement using deforming meshes," V BBVIV, Bahia, Brazil.

[2]Fisher, F. K., Gummer, J. H.,1994, Liess, C,m "Stayvane vibrations in the Nkula Falls turbines," Hydropower & Dams.

[3]Gummer, J. H., Hensman, P.C., August 1992, "A review of stayvane cracking in hydraulic turbines", Water Power & Dam Construction, pp. 32-42.

[4]Gunnar, H., Olberts, D. R., "Influence of Trailing-Edge Geometry on Hydraulic-Turbine-Blade Vibration Resulting from Vortex excitation," Journal of Basic Engineering, ASME.

[5]J. H. Gerrard, 1966, "The mechanics of the formation region of vortices behind bluff bodies," J. Fluid Mech. 25 no. Part 2, pp. 401-413.

[6]Khalak, A. Williamson C. H. K., 1999, "Motions, forces and mode transitions in vortex-induced vibrations at low mass-damping," J. Fluid and Structures 13, pp. 813-851.

[7]Liess, C., "Flow induced stress fluctuations in stay vanes of large hydraulic turbines," International Conference on Flow Induced Vibrations, England.

[8]Miyagawa,K., Fukao, S., Kawata, Y.,2004, "Study on stay vane instability due to Vortex shedding," 22th IAHR Symposium on Hydraulic Machinery and Systems, Stockholm.

[9]Gissoni, H.C., 2005, "Análise mecânica de vibrações em travessas do pré-distribuidor de turbinas hidráulicas," Department of Mechanical Engineering, University of São Paulo, MsC Thesis.

[10]Meneghini, J. R., 2002, "Projetos de pesquisa no tópico geração e desprendimento de vórtices no escoamento ao redor de cilindros," Livre-Docência, Department of Mechanical Engineering, University of São Paulo.

[11]Saltara,F., 1999, "Simulação numérica do escoamento ao redor de cilindros," Doctoral Thesis, Department of Mechanical Engineering, University of São Paulo.

[12]Chen, Y. N., "Behavior of Karman Vortex Streets Shed by Plates," Research Laboratory for Vibration and Acoustics, Sulzer Brothers Limited, Switzerland.

[13]Blevins, R. D., 1990, "Flow-induced vibration," 2nd ed., Van Nostrand Reinhold, New York.

[14]Wilcox,D.C., 1994, "Turbulence Modeling for CFD," DCW Industries Inc., California.